Self-Exchange Velocities in Molten Equimolar Li(Cl, Br) Predicting an Anion Chemla Effect

Shipra Baluja, Akira Endoh, and Isao Okada

Department of Electronic Chemistry, Tokyo Institute of Technology, Nagatsuta, Midori-ku, Yokohama 227, Japan

Z. Naturforsch. **43a,** 1065–1071 (1988); received September 25, 1988

A molecular dynamics simulation of an equimolar mixture of LiCl and LiBr melts has been performed at about 1000 K to evaluate the self-exchange velocities (SEV). The SEV of Li^+–Br^- pairs is greater than that of Li^+–Cl^- pairs. Therefore in this mixture the mobility of Br^- ions may be greater than that of Cl^- ions, that is, an "anion Chemla effect" may occur. For comparison, MD simulations of pure LiCl and LiBr melts have also been performed.

Introduction

In various common anion binary melts the Chemla effect occurs [1], i.e. the mobility of the larger cation is greater than that of the smaller one at certain concentrations and temperatures.

As for the corresponding "anion Chemla effect", only in molten Ag(Cl, NO_3) several studies on the mobilities have been done, and in all studies except one the mobility of the NO_3^- ion has been found to be greater than that of the Cl^- ion [1]. Although it is impossible to define unambiguously the ionic radius of NO_3^-, its effective radius is supposed to be greater than that of Cl^-, and the anion Chemla effect would thus occur in this system. Since there exists a specially strong interaction between Ag^+ and halide ions, this system cannot form a typical example for the anion Chemla effect.

In molten Li(Cl, NO_3), the mobility of Cl^- was assumed to be smaller than that of the average mobility of NO_3^-, NO_2^- and O^{2-} at the investigated concentrations [2]. According to our preliminary results on the same system at 650 K, Cl^- is more mobile than NO_3^- at low mole fractions of LiCl ($x_{Cl} <$ ca. 0.15), whereas at higher mole fractions the opposite is the case [3].

In molten Na(F, Cl) and Na(F, Br) [4] the anion Chemla effect has not been found in the investigated range of concentrations and temperatures.

We have interpreted the (cation) Chemla effect in terms of the self-exchange velocity (SEV) of unlike ion pairs, which is strongly correlated with the internal mobility [5, 6]. If the Chemla effect is mainly caused by the difference in the interactions between two kinds of cation-anion pairs, it is expected that also in common cation binary mixtures the anion Chemla effect occurs.

An orthodox way for calculating internal mobilities in additive binary melts by MD simulation has been presented by Klemm [7]. This method, however, still needs extensive computer time.

Thus, the main purpose of the present study was to calculate SEV's by MD simulation of a halide mixture with a common alkali ion, and to see if the results suggest the existence of a corresponding anion Chemla effect. As an example, an equimolar mixture of LiCl and LiBr melts has been chosen. For comparison, SEV's of pure LiCl and LiBr melts have also been calculated.

Reprint requests to Professor Isao Okada, Department of Electronic Chemistry, Tokyo Institute of Technology, Nagatsuta 4259, Midori-ku, Yokohama 227, Japan.

Molecular Dynamics Simulation

For our 3 systems, 432 ions were placed in the periodic cube; for the equimolar mixture, these were 216 Li^+, 108 Cl^- and 108 Br^- ions. The edge lengths L of the cubes were calculated from the data on the densities [8, 9]. The pair potentials of Tosi and Fumi [10] were adopted:

$$u_{ij}(r) = z_i z_j e^2/4\pi\varepsilon_0 r + A_{ij} b \exp[(\sigma_i+\sigma_j-r)/\varrho] - c_{ij}/r^6 - d_{ij}/r^8, \quad (1)$$

where z is the charge number, e the elementary charge, ε_0 the permittivity of vacuum, and the parameters are given in Table 1. For the mixture the combination rule presented by Larsen et al. [11] was employed. The Ewald method [12] was used for the calculation of the

0932-0784 / 88 / 1200-1065 $ 01.30/0. – Please order a reprint rather than making your own copy.

Table 1. The parameters used for the MD simulations.

	Li–Li	Cl–Cl	Br–Br	Li–Cl	Li–Br	Cl–Br	System	ϱ/pm	L/pm	Ref.
A	2.00	0.75	0.75	1.375	1.375	0.75	LiCl	34.2	2187.9	[8]
σ/pm	163.2	317.0	343.2	240.1	253.2	330.1	LiBr	35.3	2345.3	[8]
$c/10^{-79}$ J m^6	0.073	111.0	185.0	2.00	2.50	143.0	Li(Cl, Br)	34.8	2274.8	[9]
$d/10^{-99}$ J m^8	0.030	223.0	423.0	2.40	3.30	307.1				

$b = 0.338 \times 10^{-19}$ J.

Table 2. Calculated temperature, pressure and potential energy.

	LiCl	LiBr	Li(Cl, Br)
T/K	1007	1003	991
P/MPa	220	210	180
E/kJ mol^{-1}	−796.8	−747.0	−772.3

Table 3. Characteristic values of the pair correlation functions. R_1 and R_2 are the distances where $g_{ij}(r)$ crosses unity for the first and the second time, respectively. R_M and R_m are the distances at the first maximum and the first minimum, respectively. The values in parentheses are equivalent coordination numbers within R_2.

	R_1	R_M	$g(R_M)$	R_2/pm	R_m/pm	$g(R_m)$
LiCl						
Li–Li	318	371	1.82	459	535	0.69
Cl–Cl	324	373	2.13	455	537	0.65
Li–Cl	192	223	3.72	281 (3.09)	353	0.46
LiBr						
Li–Li	341	397	1.79	494	573	0.70
Br–Br	348	401	2.14	487	573	0.63
Li–Br	207	239	3.78	303 (3.10)	369	0.47
Li(Cl, Br)						
Li–Li	327	385	1.80	477	553	0.72
Cl–Cl	323	369	2.19	455	527	0.62
Br–Br	350	397	2.13	491	577	0.65
Li–Cl	188	219	4.29	279 (3.02)	353	0.42
Li–Br	211	241	3.40	304 (3.18)	367	0.50
Cl–Br	335	381	2.14	469	551	0.63

Coulomb force; the cut length in the real space was set as $L/2$, the vector in the reciprocal space was taken up to 27, and the parameter α was set so that $\alpha L = 5.6$. The constant energy procedure was employed. The time step was 4 fs.

After equilibrium, the configurations for about 5000 steps were employed for the calculation of several properties for the systems. The calculated temperatures, pressures and potential energies are listed in Table 2.

Results and Discussion

Pair Correlation Functions

The characteristic values of the pair correlation functions $g(r)$ are given in Table 3. Figure 1 shows the $g(r)$'s and the equivalent running coordination numbers n^e, which will be explained later, for the unlike ion pairs. The positions of the first maximum R_M of g_{LiCl} and g_{LiBr} for the mixture are nearly equal to those for the pure salts, respectively, while the peak heights increase with increasing concentration of LiBr. Similar behaviour has been observed in MD simulations of common anion binary mixtures such as (Li, K)Cl [6, 13, 14], (Li, K)Br [15], and (Li, Rb)Cl [5]. This can be explained in the present case as follows. As the concentration of LiBr increases, the average distance between two neighbouring Li^+ ions increases, as seen also from the positions of the first maximum of $g_{LiLi}(r)$ in Table 3. The halide ions are more associated with the nearest neighbouring Li^+ ions by experiencing less interference from other surrounding Li^+ ions.

Coordination Numbers

The running coordination numbers of j about i is defined as

$$n_{ij}(r) = 4\pi \varrho_j \int_0^r r'^2 g_{ij}(r')\, dr', \qquad (2)$$

where ϱ_j is the average number density of species j. The equivalent running coordination number $n^e_{ij}(r)$ is defined as $n^e_{ij}(r) = n_{ij}(r)/x_j$ (x_j is the mole fraction of species j).

As seen from Fig. 1, $n^e(r)$ at short distances becomes greater with increasing concentration of LiBr, whereas the opposite trend is observed at longer distances. When the mixture is compared with the pure salts, the crossing points are found at 267 pm for Li–Cl and 290 pm for Li–Br. This corresponds to what was explained above: as the concentration of LiBr increases, the halide ions are more coordinated by Li^+ in the

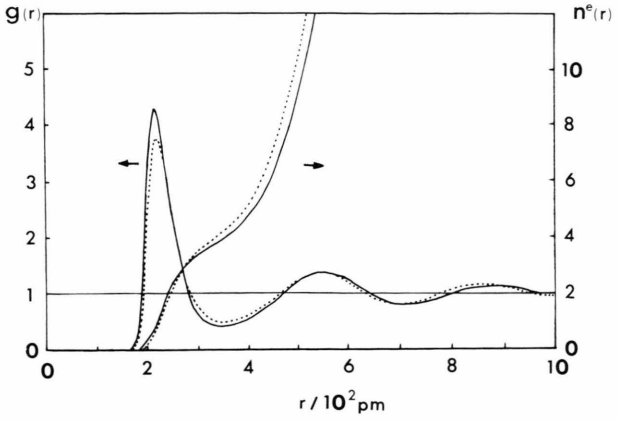

(a)

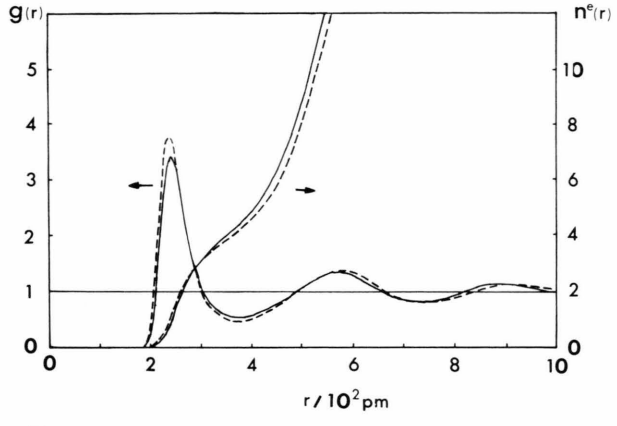

(b)

Fig. 1. Pair correlation functions $g(r)$ and equivalent coordination numbers $n^e(r)$ for (a) Li^+-Cl^- pairs and (b) Li^+-Br^- pairs. —— Mixture, ····· pure LiCl, – – – pure LiBr.

Table 4. Percentage of simultaneous coordination numbers of Cl^- and Br^- ions to a Li^+ ion. The coordination area is defined as the distances within R_2, that is, 279 pm for Cl^- and 304 pm for Br^-.

Cl \ Br	0	1	2	3	4	5	Total
0	0	0.28	3.44	7.03	2.40	0.07	13.22
1	0.36	8.54	21.33	7.48	0.21	0.00	37.92
2	4.94	20.54	9.11	0.28	0.00	0	34.87
3	6.90	5.48	0.22	0.00	0.00	0	12.60
4	1.28	0.09	0	0	0	0	1.37
5	0.02	0	0	0	0	0	0.02
Total	13.50	34.93	34.10	14.79	2.61	0.07	100.00

immediate vicinity, while farther away the number density of the Li^+ ions decreases. $n^e(r)$ at $r = R_2$ is given in Table 3; R_2 may be regarded as the end of the nearest neighbour interaction [16].

Table 4 gives the percentage of simultaneous Cl^- and Br^- coordination numbers to a Li^+ ion in the mixture. As the limit of the coordination sphere the values of R_2 are chosen here, that is, 279 pm for Li^+-Cl^- pairs and 304 pm for Li^+-Br^- pairs. A combination of the coordination number 1 for Cl^- and 2 for Br^- is most probable (21.33%), and a combination of 2 for Cl^- and 1 for Br^- is almost equally probable (20.54%).

Angular Correlation

For further insight into the short range structure, the angular correlation function

$$P_{-+-}(\theta) = C\, \mathrm{d}n(\theta)/(\sin\theta\, \mathrm{d}\theta) \tag{3}$$

has been calculated, where C is the normalisation constant taken so that $\int_0^{180^\circ} P_{-+-}(\theta)\, \mathrm{d}\theta = 1$, and $\mathrm{d}n(\theta)$ is the number of Cl^- (or Br^-) ions around a Li^+ ion within the distance R_2 between $\theta - \Delta\theta/2$ and $\theta + \Delta\theta/2$ ($\Delta\theta = 1^\circ$). $P_{-+-}(\theta)$'s in the pure salts and the mixture are shown in Figure 2. The first peak positions are located around 102° in all the cases. This indicates that with high probability Li^+ ions are coordinated by the halide ions nearly regular-tetrahedrally.

Figure 2 reveals that these curves become slightly flatter with increasing concentration of LiBr. This is probably due to the large repulsive force between a Br^- ion and other Cl^- or Br^- ions surrounding the same Li^+ ion.

Figure 3 shows $P_{+-+}(\theta)$. The concentration dependence of $P_{+-+}(\theta)$ is rather great, in contrast with $P_{-+-}(\theta)$; as the concentration of LiBr increases, Li^+ ions become more structured around Cl^- or Br^- ions. The $P_{+-+}(\theta)$'s for $\measuredangle$ Li–Cl–Li have the maximums at 100° and 106° in pure LiCl and the mixture, respectively, while those for $\measuredangle$ Li–Br–Li have the maximums at 102° in both pure LiBr and the mixture.

The repulsive force between the halide ions surrounding a Li^+ ion is generally greater than that between Li^+ ions coordinating to a Cl^- (or Br^-) ion, and thereby the curves of $P_{+-+}(\theta)$ are flatter than those of $P_{-+-}(\theta)$.

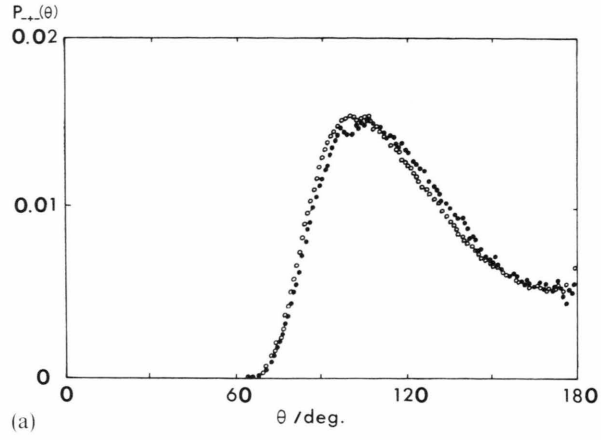

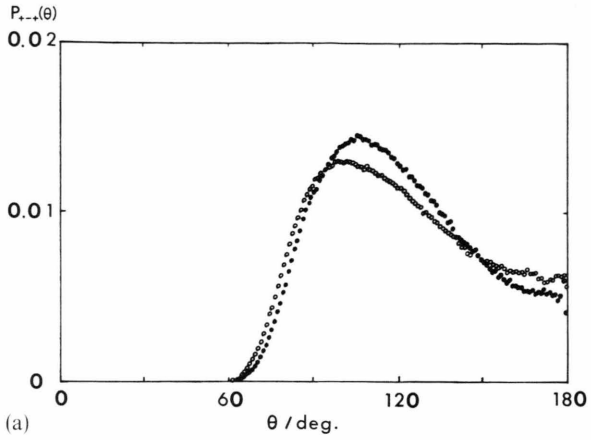

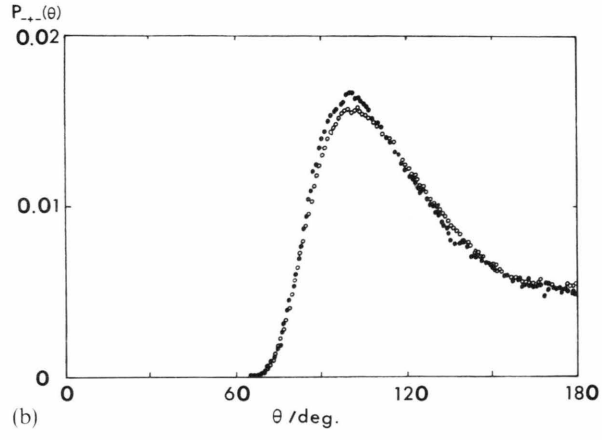

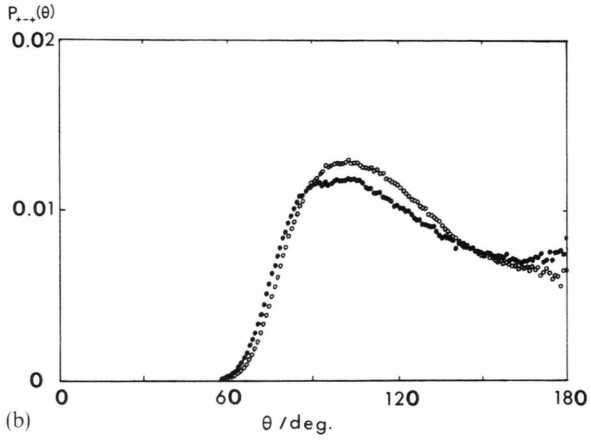

Fig. 2. Angular correlation functions $P_{-+-}(\theta)$ for
(a) ∢ Cl–Li–Cl and
(b) ∢ Br–Li–Br. • The mixture, ○ pure LiCl or LiBr.

Fig. 3. Angular correlation functions $P_{+-+}(\theta)$ for
(a) ∢ Li–Cl–Li and
(b) ∢ Li–Br–Li. • The mixture, ○ pure LiCl or LiBr.

System	Li–Cl ($m\,s^{-1}$)	Li–Br ($m\,s^{-1}$)
LiCl	145	–
LiBr	–	120
Li(Cl, Br)	119	134

Table 5.
The self-exchange velocity of neighbouring unlike ions at about 1000 K.

Self-Exchange Velocities

The average velocity of the separating motion of unlike ion pairs can be expressed in terms of the self-exchange velocity (SEV), which is defined by [5]

$$v = (R_2 - \bar{R}_2)/\tau, \tag{4}$$

where $\bar{R}_2$ is the average distance between Li^+ and Cl^- (or Br^-) ions located within R_2 of the Li^+ ions. The anions in question within the distance R_2 from each Li^+ ion are marked. With the lapse of time, the marked anions move to R_2. The average time needed for this movement is τ.

The values of v for Li^+-Cl^- and Li^+-Br^- pairs are given in Table 5. In the mixture, the SEV of Li^+-Br^- pairs is greater than that of Li^+-Cl^- pairs.

Figure 4 shows the relationship between SEV and internal mobility in the melts so far studied. In view of this good correlation, the mobility of Br^- is expected to be greater than that of Cl^- ions in the present equimolar mixture. That is, the anion Chemla effect is expected to occur in this mixture.

Figure 5 gives examples of the time evolution of distances of individual Cl^- and Br^- ions located within the respective R_2's at $t = 0$ from an arbitrarily chosen Li^+ ion. This kind of motion can be classified

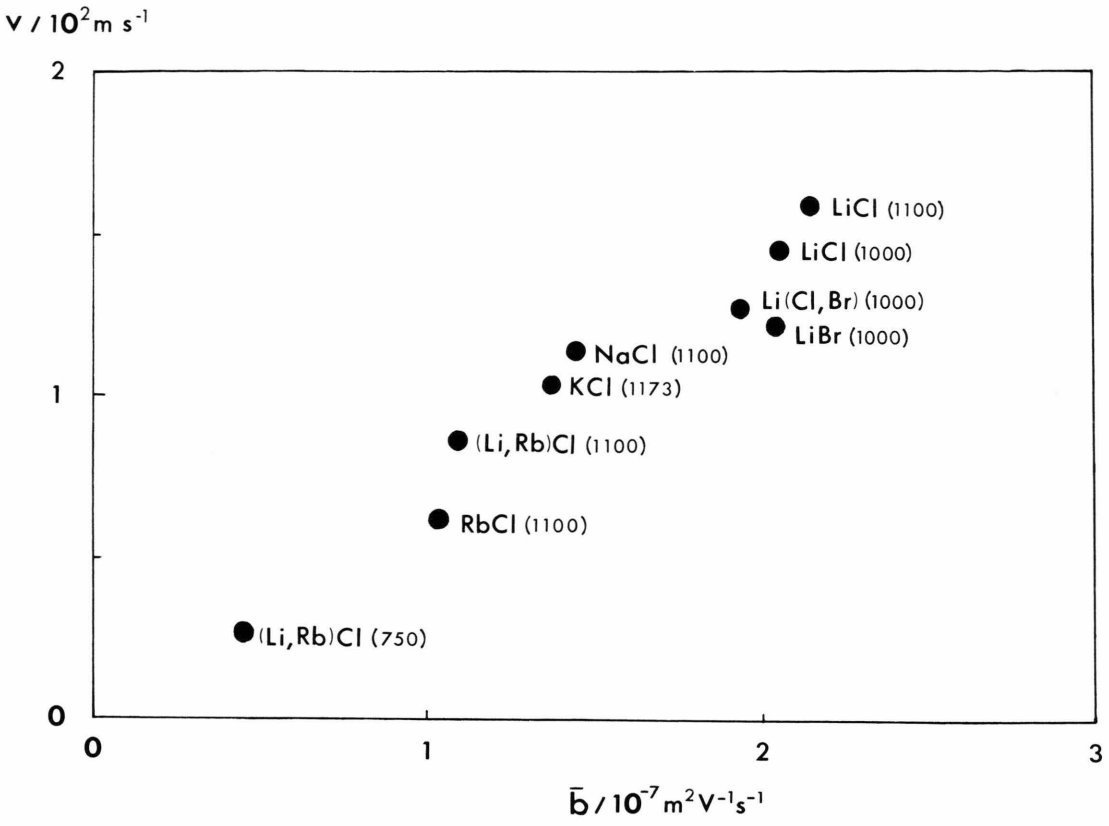

Fig. 4. Relationship between SEV (v) and internal mobility (b). The mixtures given here are equimolar, and for them average values of v and b are plotted. The values in parentheses refer to temperatures in K. The SEV's are taken from the following references: LiCl (1100) [5], KCl [19], RbCl [5], and (Li, Rb)Cl [5]. The value for NaCl is an unpublished one.

into four modes [6]: oscillating motion (O-process) [17], leaving motion (L-process), wandering motion (W-process), and coming back motion (C-process).

The average duration of the O-process for Cl^- and Br^- ions in the mixture and the pure salts is compared in Fig. 6, which shows the percentage of the anions terminating the O-process within the time given on the abscissa. The unsmoothness of the curves is due to the statistical errors. As seen from Fig. 6, in the mixture the O-process of Cl^- lasts longer than that of Br^-. This shows that in the mixture the Cl^- ions are more associated with the nearest neighbouring Li^+ ions than the Br^- ions. Figure 6 reveals that the sequence of the time needed for the O-process in the 4 cases coincides with the inverse sequence of the SEV's.

In a previous study, we have found an empirical relation for the average velocity of the separating motion in the L-process [6]:

$$v_L = (0.577 \pm 0.005)(v_c + v_a), \tag{5}$$

where v_c and v_a are the average velocities of the ideal-gas like cations and anions, respectively, i.e., $v_c = \sqrt{8RT/\pi M_c}$ and $v_a = \sqrt{8RT/\pi M_a}$ (M_c and M_a are the molar masses of the cation and the anion, respectively). In Table 6 the v_L values in the present systems are given together with those calculated from (5). Table 6 shows that also in the present systems the v_L values are equal to those expressed by (5) within the statistical errors. In the L-process the Cl^- ions are thus faster than the Br^- ions.

Anion Chemla Effect

In the present equimolar mixture, the SEV of Br^- is greater than that of Cl^-. This suggests that in the

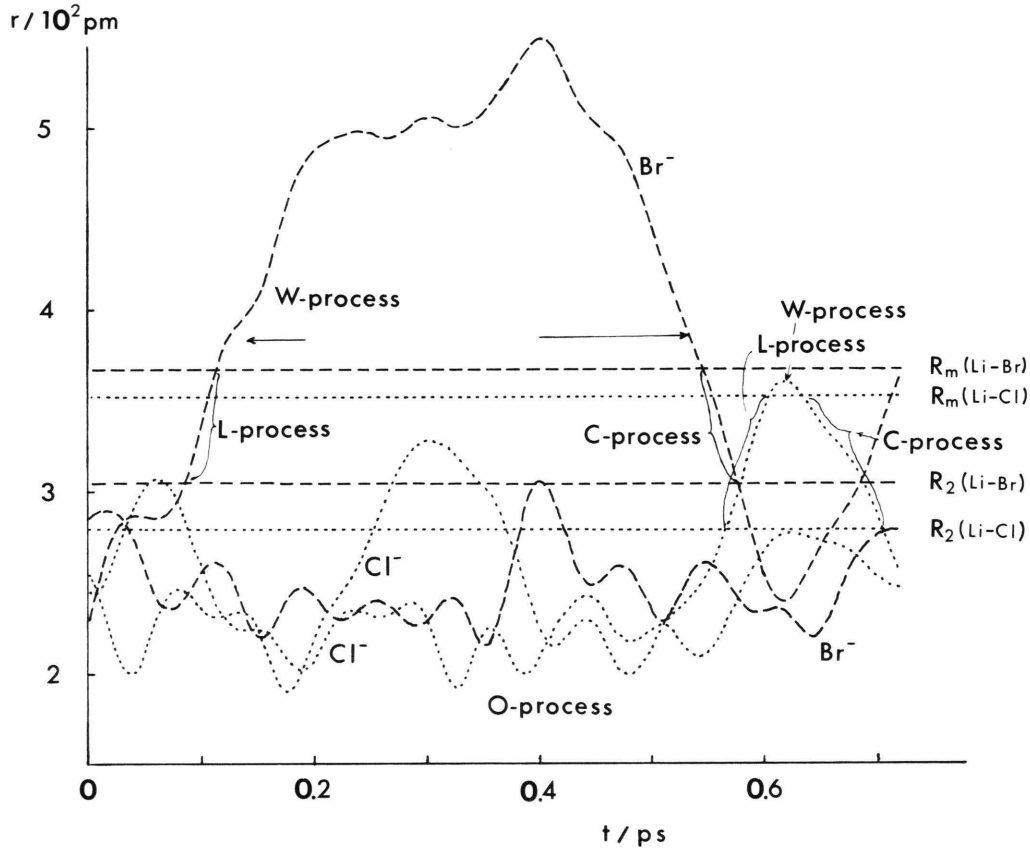

Fig. 5. Examples of the time evolution of distances of Cl^- and Br^- ions located within the respective R_2's at $t = 0$ from a Li^+ ion. O: oscillating, L: leaving, W: wandering, C: coming back. ···· Cl^-, ––– Br^-.

Table 6. The velocity of the separating motion in the L-process. The values in brackets are those obtained from (5).

System	Li–Cl ($m\,s^{-1}$)	Li–Br ($m\,s^{-1}$)
LiCl	1404 ± 23 [1457 ± 13]	
LiBr		1346 ± 23 [1307 ± 12]
Li(Cl, Br)	1484 ± 36 [1447 ± 13]	1329 ± 30 [1299 ± 12]

Table 7. The self-diffusion coefficients at about 1000 K. The values in brackets are the experimentally obtained ones at 1000 K under ambient pressure [18].

System	Li^+	Cl^-	Br^-
		($10^{-9}\,m^2\,s^{-1}$)	
LiCl	11.8 ± 0.5	7.4 ± 0.1	
	[14.2 ± 0.8]	[7.2 ± 0.3]	
LiBr	9.0 ± 0.2		5.1 ± 0.4
Li(Cl, Br)	9.2 ± 0.1	7.6 ± 0.2	8.6 ± 0.1

mobilities the anion Chemla effect may occur. At higher concentration of LiBr and/or higher temperature, the relative difference in the mobilities of Br^- and Cl^- ions will become greater, that is, the anion Chemla effect will become more pronounced.

The ionic radii of anions X are relatively large except for a few anions such as H^-. The relative difference in the pair potential minima between $M-X_1$ and $M-X_2$ is hence generally small except in the case that M is a multivalent cation or a small cation such as Li^+ ion. The anion Chemla effect may not occur except in such cases.

Self-Diffusion Coefficients

The self-diffusion coefficients D in the mixture and the pure melts have been evaluated from the mean

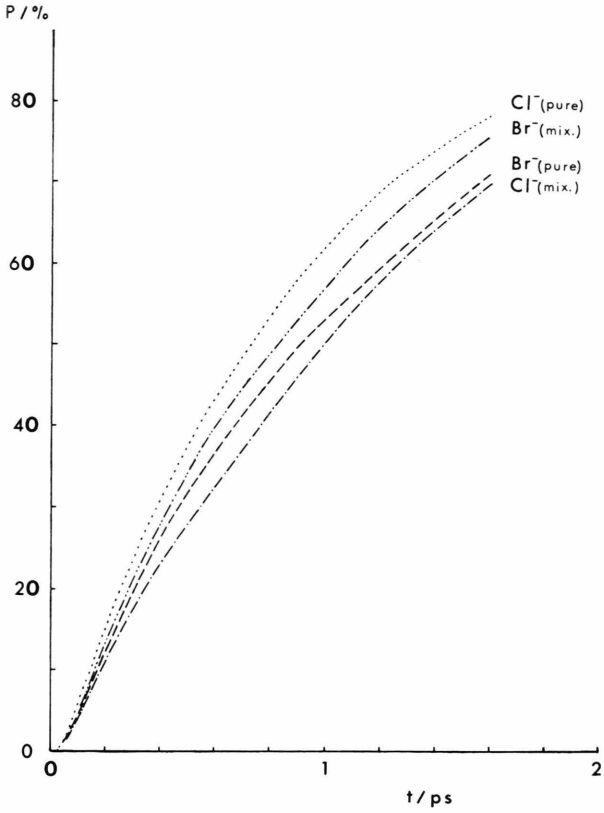

Fig. 6. Percentage of the anions terminating the O-process within the time given on the abscissa.

square displacements, which have been taken over 14 ps from 50 different time origins. The calculated values are given in Table 7 together with the experimental values for pure LiCl [18]. In the following discussions it should be borne in mind that the self-diffusion coefficients cannot so precisely be calculated as the SEV's.

In the mixture, D_{Br} seems to be greater than D_{Cl}. This is presumably because in the mixture the Cl^- ions are more associated than the Br^- ions.

D_{Li} becomes smaller with increasing concentration of LiBr; this is probably because the Li^+ ions become more associated. D_{Cl} in pure LiCl and the mixture is nearly equal. The decrease of D_{Cl} with increasing association may be compensated by the motion of the slightly more active Br^- ions.

D_{Br} in pure LiBr is smaller than that in the mixture, although the free space may be greater in the former than in the latter. This may also be due to the association being more pronounced in the latter, as seen from the SEV's.

In conclusion, in the equimolar mixture of Li(Cl, Br) at about 1000 K, the SEV of Br^- ions is greater than that of Cl^- ions. This suggests that in this mixture the mobility of Br^- ions may be greater than that of Cl^- ions, and thus, the Chemla effect will occur also in common cation binary mixtures. Experimental substantiation is under progress.

One of us (S.B.) wishes to thank the Ministry of Education, Science and Culture, Japan for the scholarship which financially supports her stay in Japan. The expenses of this work were partially defrayed by the Grant-in-Aid for Special Project Research (No. 62124039) from the same Ministry.

The calculation was performed with HITAC M-680 H computers at the Institute for Molecular Science at Okazaki and the High Energy Physics Institute at Tsukuba. The computer time made available for this study is gratefully acknowledged.

[1] A. Klemm, Advances in Molten Salt Chemistry 6 (G. Mamantov et al., ed.). Elsevier 1987, p. 1.
[2] V. Ljubimov and A. Lundén, Z. Naturforsch. **30a,** 75 (1975).
[3] A. Endoh and I. Okada, to be published.
[4] K. Grjotheim, O. Haugerød, H. Stamnes, and H. A. Øye, Electrochim. Acta **17,** 1547 (1972).
[5] I. Okada, R. Takagi, and K. Kawamura, Z. Naturforsch. **35a,** 493 (1980).
[6] I. Okada, Z. Naturforsch. **42a,** 21 (1987).
[7] A. Klemm, Z. Naturforsch. **32a,** 927 (1977).
[8] G. J. Janz, F. W. Dampier, G. R. Lakshminarayanan, P. K. Lorenz, and R. P. T. Tomkins, Molten Salts: Vol. 1, Electrical Conductance, Density, and Viscosity Data, NSRDS-NBS **15,** Nat. Bur. Stand., Washington 1968.
[9] G. J. Janz, R. P. T. Tomkins, and C. B. Allen, Phys. Chem. Ref. Data **8,** 125 (1979).
[10] M. P. Tosi and F. G. Fumi, J. Phys. Chem. Solids **25,** 45 (1964).
[11] B. Larsen, T. Førland, and K. Singer, Mol. Phys. **26,** 1521 (1973).
[12] P. P. Ewald, Ann. Phys. **64,** 253 (1921).
[13] C. Caccamo and M. Dixon, J. Phys. C: Solid Stat. Phys. **13,** 1887 (1980).
[14] F. Lantelme and P. Turq, J. Chem. Phys. **77,** 3177 (1982).
[15] F. Lantelme and P. Turq, Mol. Phys. **38,** 1003 (1979).
[16] G. Pálinkás, W. O. Riede, and K. Heinzinger, Z. Naturforsch. **32a,** 1137 (1977).
[17] In [6], as the definition of the O-process, the italic part was missing: The cation starts within R_2 at the time $t = 0$ and passes R_m for the first time *after passing* R_2 *for the last time* at the time t.
[18] R. Lenke, W. Uebelhack, and A. Klemm, Z. Naturforsch. **28a,** 881 (1973).
[19] R. Takagi, I. Okada, and K. Kawamura, Z. Naturforsch. **36a,** 1106 (1981).